OUTSTANDING MEETING PAPER

Papers in this section are based on submissions to the MRS Symposium Proceedings that were selected by Symposium Organizers as the outstanding paper. Upon selection, authors are invited to submit their research results to Journal of Materials Research. *These papers are subject to the same peer review and editorial standards as all other JMR papers. This is another way by which the Materials Research Society recognizes high quality papers presented at its meetings.*

Review

Phase change materials: From structures to kinetics

Wojciech Wełnic,[a] Johannes A. Kalb,[b] Daniel Wamwangi, Christoph Steimer, and Matthias Wuttig
I. Physikalisches Institut (IA), Rheinisch-Westfâlisch Technische Hochschule (RWTH) Aachen University of Technology, 52056 Aachen, Germany

(Received 19 January 2007; accepted 2 May 2007)

Phase change materials possess a unique combination of properties, which includes a pronounced property contrast between the amorphous and crystalline state, i.e., high electrical and optical contrast. In particular, the latter observation is indicative of a considerable structural difference between the amorphous and crystalline state, which furthermore is characterized by a very high vacancy concentration unknown from common semiconductors. Through the use of ab initio calculations, this work shows how the electric and optical contrast is correlated with structural differences between the crystalline and the amorphous state and how the vacancy concentration controls the optical properties. Furthermore, crystal nucleation rates and crystal growth velocities of various phase change materials have been determined by atomic force microscopy and differential thermal analysis. In particular, the observation of different recrystallization mechanisms upon laser heating of amorphous marks is explained by the relative difference of just three basic parameters among these alloys, namely, the melt-crystalline interfacial energy, the entropy of fusion, and the glass transition temperature.

I. INTRODUCTION

Phase change materials are very promising materials for information technology. They are already used in rewriteable optical data storage, where the pronounced difference of optical properties between the amorphous and crystalline state is used for data storage. This unconventional class of materials is also the basis of storage concepts for replacement flash memories.[1-6] This raises the question of which material properties are crucial for these storage applications and which compounds posses the required properties. Successful phase change alloys are characterized by a unique property combination. On the one hand, they possess a pronounced contrast of optical properties (reflectivity, transmission) between the amorphous and crystalline state. Figure 1 shows a comparison of (b) the imaginary part of the dielectric function for GeTe, a prototype phase change alloy, in comparison with (a) the corresponding spectrum of GaAs. The pronounced optical contrast displayed in GeTe is a unique and rather rare property. Conventional semiconductors such as GaAs or Si are characterized by a much smaller difference in optical properties. Therefore, we need to understand what causes the property contrast in phase change alloys. The only plausible explanation is a considerable structural difference between the amorphous and crystalline state. Such a different atomic arrangement could lead to different electronic states, which should give rise to different optical properties.

II. STRUCTURE AND PROPERTIES

In the following, we will discuss the structural properties of phase change alloys. However, optical contrast alone is not sufficient. In data storage speed, for example,

[a] Address all correspondence to this author.
Present address: Laboratoire des Solides Irradiés, CNRS-CEA, École Polytechnique, Palaiseau, France, European Theoretical Spectroscopy Facility (ETSF).
e-mail: welnic@physik.rwth-aachen.de
[b] Present address: Massachusetts Institute of Technology, Department of Materials Science and Engineering, Cambridge, MA 02139.
This paper was selected as the Outstanding Meeting Paper for the 2006 MRS Spring Meeting Symposium M Proceedings, Vol. 918.
DOI: 10.1557/JMR.2007.0301

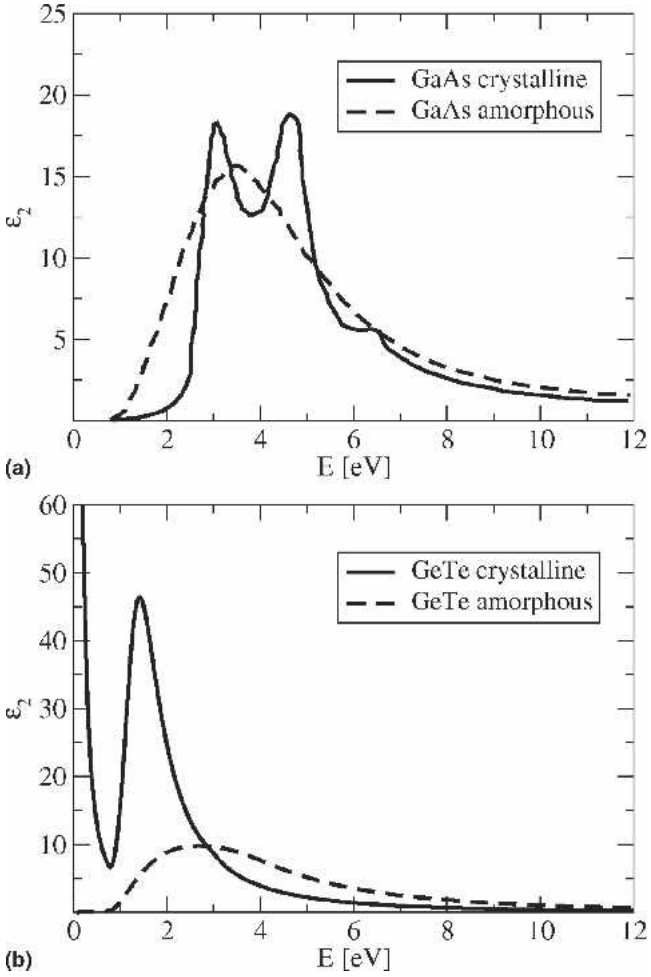

FIG. 1. Imaginary part of the dielectric constant ϵ_2 for (a) GaAs[7,8] and (b) GeTe,[9] a prototype phase change material, in the amorphous and crystalline states. Note the pronounced difference in amplitude in GeTe compared to GaAs and the larger band gap in the amorphous state.

fast structural rearrangements are also required. In phase change recording, crystallization times of a few nanoseconds have indeed been observed. While fast crystallization alone is not uncommon and certain materials are known for their fast crystallization processes, it is more difficult to understand how crystallization can be fast in materials where the atomic arrangement in the amorphous and crystalline state is very different. In the following, we will therefore start by discussing the structural properties of typical phase change alloys.

Recently Kolobov et al. provided extended x-ray absorption fine structure (EXAFS) data for GeTe and $Ge_2Sb_2Te_5$, which reveal a structural difference between the amorphous and crystalline states.[10,11] The most noteworthy structural change is a rearrangement of the Ge atom from an octahedral site in the crystalline state to a tetrahedral site in the amorphous state. We have therefore used density-functional theory to determine the relationship between structure and energy for a typical phase change alloy.[13] Luo et al. have already shown that density-functional theory can be successfully used for phase change materials and predicted that suitable alloys should exhibit a rocksalt structure and a number of s- and p-valence electrons of more than four.[14] For our calculations, we have used $Ge_1Sb_2Te_4$. To determine the atomic arrangement in $Ge_1Sb_2Te_4$, a number of different atomic arrangements have been considered. They include the chalcopyrite structure, where every atom is tetrahedrally coordinated, the rocksalt phase, and the spinel structure, where Ge has four nearest neighbors and Sb and Te are octahedrally coordinated. All structures have been calculated in supercells containing 56 atoms. The resulting energy as a function of lattice size is displayed in Fig. 2. It can be seen that the chalcopyrite structure has a much larger lattice constant leading to a volume increase of 30% compared to the rocksalt phase. As such a large increase in volume is not found experimentally, this phase will not be adopted in phase change alloys. The lowest energy is found for a distorted rocksalt structure where shorter and longer Ge–Te as well as Sb–Te bonds are formed. Such a distortion pattern is characteristic for a Peierls-like distortion.[15] The atomic arrangement with second-lowest energy is found for the spinel structure, where Ge atoms have a tetrahedral coordination. This is in line with the EXAFS analysis by Kolobov et al.,[11] who observed a tetrahedral arrangement of Ge atoms in the amorphous state. The density of this phase is lower, as can be seen from Fig. 2. The quantitative difference between these two phases is around 30 meV, in good agreement with the observed heat of crystallization.[12] Note that the spinel structure we use to model the amorphous

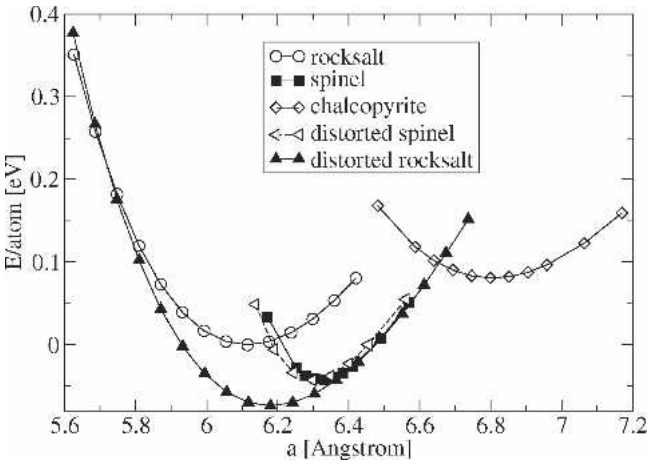

FIG. 2. Ground-state energy versus lattice constant for the undistorted and distorted rocksalt, spinel, and chalcopyrite structures. Due to its negligible energetic and structural relaxation, only the ideal chalcopyrite values are shown. The energy difference and lattice expansion between the structure with lowest energy (distorted rocksalt) and the structure with second-lowest energy, the spinel phase are in good agreement with values for the energy difference between the crystalline and amorphous phase obtained by differential scanning calorimetry.[12] (Data are from Ref. 13.)

state in the Density Functional Theory (DFT) calculations still possesses long-range order, since the calculations are performed within a unit cell containing 56 atoms. Yet the pronounced optical contrast that is characteristic for phase change alloys must be related to differences in the short range order between the amorphous and crystalline states. Such differences can be reasonably well described employing medium size unit cells. Hence the most pronounced difference between the two phases, i.e., the distorted rocksalt structure describing the metastable crystalline state and the spinel structure describing the atomic arrangement in the amorphous structure, is the arrangement of the Ge atoms. However, the electronic states of germanium do not exhibit major changes upon the crystalline-amorphous phase transition, as illustrated by Fig. 3. Here the difference in the density of states between the rocksalt and the spinel structure is displayed. It is noteworthy that a significant change of states is observed close to the Fermi energy. This change is mainly caused by differences in the p-states of Te, even though Ge atoms are shifted the most if we compare the arrangement in the rocksalt and spinel structure. Another interesting feature in GeSbTe alloys is the unusually high vacancy concentration in the crystalline state. $Ge_1Sb_2Te_4$ exhibits 25% of its vacancies on the Ge/Sb sublattice, while in $Ge_2Sb_2Te_5$, 20% of the lattice sites remain unoccupied.[16–18] Here we investigate the role of composition for "GeSbTe" alloys by a computational approach, namely by investigating systems with varying amounts of Ge, Sb, and Te vacancies using ab initio density-functional theory. We start with a hypothetical $Ge_2Sb_2Te_4$ alloy with a rocksalt structure and a total number of 64 atoms (16 atoms of Ge and Sb each, 32 atoms of Te) in the computational supercell and subsequently remove Ge and Sb atoms. As recent experiments, as well as theoretical calculations, have found evidence that the rocksalt structure is accompanied by considerable distortions around the ideal atomic positions in GeSbTe alloys,[11,13,15] we further relax the structures. The formation energies of the obtained stoichiometries are then calculated using the following equation:

$$\Delta E = [E_v + n_v E(\mathrm{Ge/Sb})] - E(Ge_2Sb_2Te_4) \quad . \quad (1)$$

Here $E(Ge_2Sb_2Te_4)$ and E_v denote the total energies of the supercells with the original composition $Ge_2Sb_2Te_4$ and of the composition resulting from the removal of Ge or Sb atoms, respectively. E(Ge/Sb) is the energy of the respective crystalline reservoir of Ge or Sb while n_v denotes the number of vacancies created upon the removal of the atoms. The results are displayed in Fig. 4(a) for the

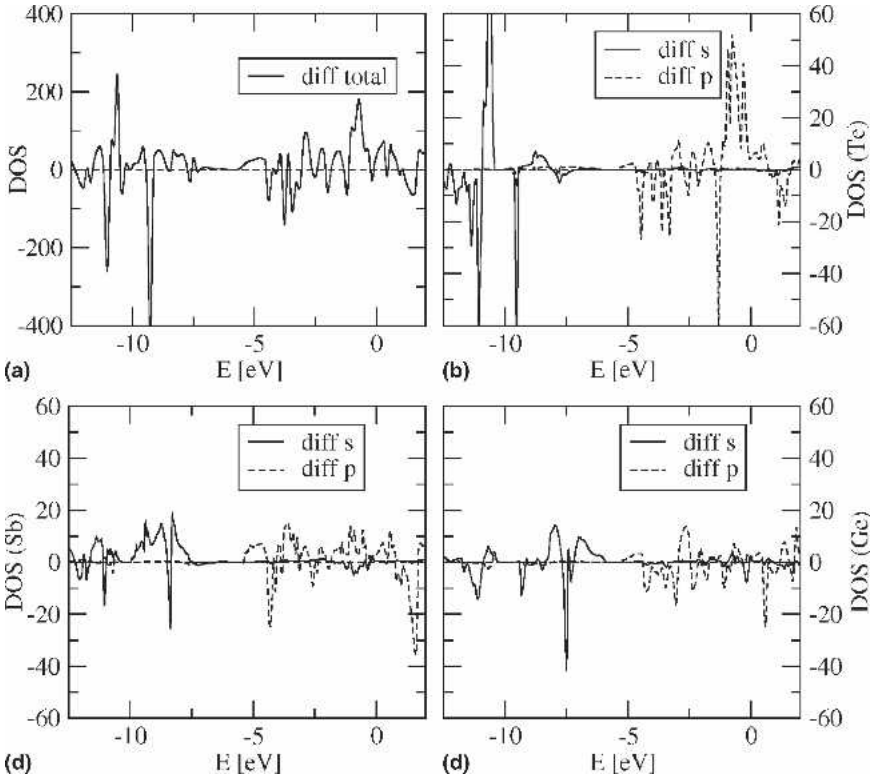

FIG. 3. Difference of the density of states (DOS) between the relaxed rocksalt and spinel structures for all atoms and for the *s* and *p* bands for each element. The difference of the overall density of states shows an increase just below the Fermi level from 0 eV ($= E_F$) down to–5 eV, which should be responsible for the optical contrast in the visible range observed on crystallization. The difference in the density of states can be attributed mostly to the *p* orbitals of Te, as Ge shows a broad change in the *s* band well below the energies relevant only for the optical properties but small differences in the *p* band. The changes in the Sb *s* and *p* band are in between the extremes Ge and Te. (Data are from Ref. 13.)

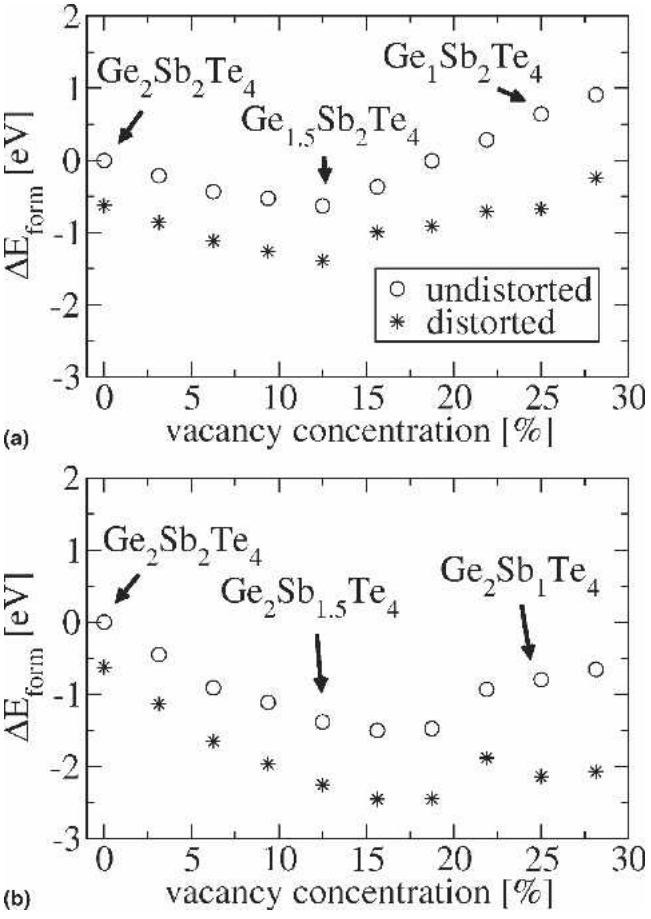

FIG. 4. Formation energies for (a) Ge and (b) Sb vacancies for different concentrations of vacancies in the Ge/Sb sublattice. The corresponding stoichiometries are marked above. Upon removing Ge atoms the energy of the crystal lowers on the order of half an electron volt per supercell. The distortions lead to a further reduction. (Data are from Ref. 16.)

removal of Ge atoms and in Fig. 4(b) for the removal of Sb atoms. Both structurally unrelaxed and relaxed (distorted) rocksalt structures are shown here. The energy of the crystal lowers upon removing Ge/Sb atoms from the $Ge_2Sb_2Te_4$ crystal such that the removal from the $Ge_2Sb_2Te_4$ crystal is energetically favorable, in striking contrast to the behavior in Si or GaAs where vacancy formation energies are large and positive (see, for example, Ref. 20). Figure 4 also shows that it is even favorable to remove several Ge atoms from the $Ge_2Sb_2Te_4$ supercell, with 4 Ge vacancies yielding a composition of $Ge_{1.5}Sb_2Te_4$. Five to six Sb vacancies are most favorable. A second point apparent from Fig. 4 is that lattice distortions also play a crucial role. They lead to a considerable further reduction in energy,[16] which is in line with earlier results by Gaspard et al.[21,22] So far, mainly alloys along the GeTe–Sb_2Te_3 pseudobinary line have been known and used in phase change recording. These calculations now lead to the prediction of novel phase change alloys with higher structural stability in the crystalline phase away from the pseudobinary line. In the following, we have experimentally produced these new alloys by sputter deposition and tested their phase change properties. The material has been deposited by direct current magnetron sputtering. The background pressure was approximately 10^{-7} mbar, and the working pressure during sputtering in Ar ambient 3×10^{-3} mbar. The sputtering power was 20 W. The as-deposited films are amorphous while the metastable crystalline phase of all the novel alloys shows the characteristic peaks of the rocksalt structure with lattice parameters of around 6 Å (Fig. 5) and no evidence for phase separation in the metastable phase. Figure 6(a) shows the absorption spectra for $Ge_1Sb_2Te_4$, $Ge_{1.5}Sb_2Te_4$, $Ge_2Sb_2Te_4$, and $Ge_2Sb_1Te_4$. While the curves are very similar in the amorphous phase, the absorption intensity increases significantly in the crystalline phase if we move from $Ge_1Sb_2Te_4$ to $Ge_{1.5}Sb_2Te_4$ and further to $Ge_2Sb_2Te_4$. The absorption spectra for $Ge_{1.5}Sb_2Te_4$ and $Ge_2Sb_1Te_4$ are similar. The optical contrast—which is of great importance for the optical data storage application of phase change materials—in the novel compositions $Ge_{1.5}Sb_2Te_4$, $Ge_2Sb_1Te_4$, and, in particular, $Ge_2Sb_2Te_4$ is therefore significantly

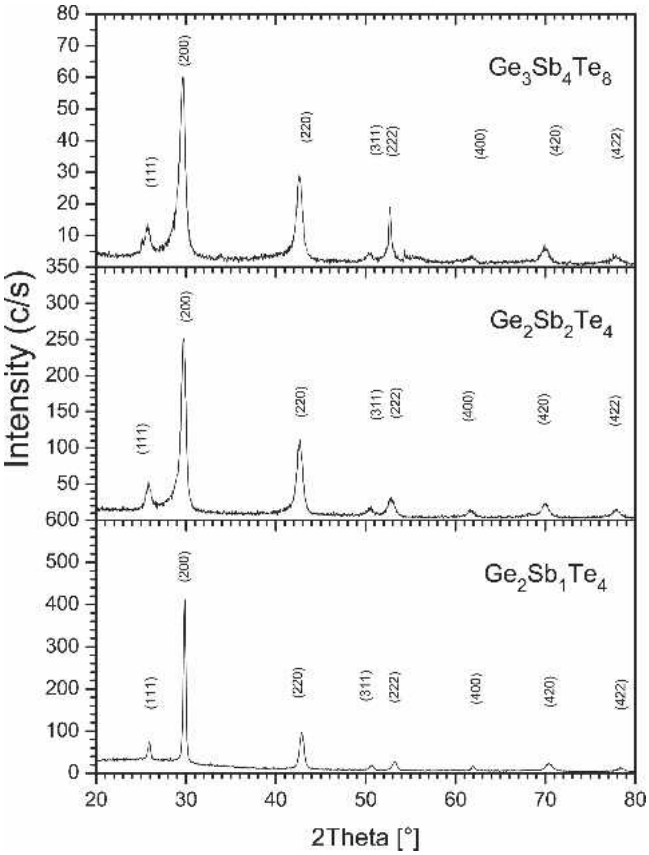

FIG. 5. XRD diffractograms of $Ge_{1.5}Sb_2Te_4$, $Ge_2Sb_2Te_4$ and $Ge_2Sb_1Te_4$. The diffractograms show a metastable phase after crystallization of the as deposited amorphous phase by annealing at 200 °C for 10 min. The peaks have been identified and attributed to the metastable rock salt structure. (Data are from Ref. 16.)

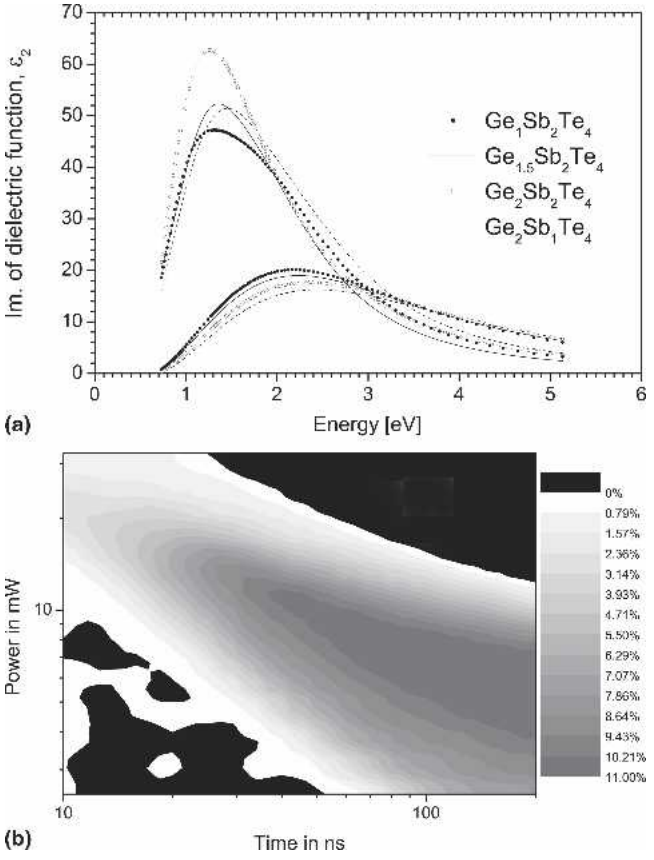

FIG. 6. Optical properties and recrystallization behavior. (a) The imaginary part of the dielectric function is presented for the amorphous (solid lines) and crystalline phases (broken lines) of the $Ge_1Sb_2Te_4$–$Ge_2Sb_2Te_4$ alloys and of $Ge_2Sb_1Te_4$. There is a systematic increase in absorption with decreasing Ge and Sb vacancy concentrations, which is consistent with the theoretical predictions. (b) Power time effect diagram to show the recrystallization of the $Ge_{1.5}Sb_2Te_4$ alloy after laser amorphization: Recrystallization leads to an increase in reflectivity. It is observed that complete recrystallization is accomplished within 30 ns, which is sufficiently fast. (Data are from Ref. 16.)

more pronounced than in $Ge_1Sb_2Te_4$. As the vacancy concentration decreases when moving from $Ge_1Sb_2Te_4$ to $Ge_{1.5}Sb_2Te_4$ and further to $Ge_2Sb_2Te_4$, the data show a clear trend toward increasing optical contrast for a decreasing number of vacancies. Such a stoichiometric trend is of tremendous interest for the application of these materials in optical data storage.

The suitability of any phase change alloy is determined also by the rapid and reversible phase transformation. The time limiting step in optical recording is recrystallization,[2] which was investigated for all new alloys. In Fig. 6(b), we present the recrystallization results of the $Ge_{1.5}Sb_2Te_4$ alloy. It is clearly seen that complete recrystallization proceeds after 30 ns, and this is comparable to the values of the widely used $Ge_2Sb_2Te_5$ alloy (10 ns). Thus the new alloys exhibit properties similar or even superior to those of conventional phase change alloys found along the pseudobinary line.

III. KINETICS

As discussed above, phase change alloys are characterized by a unique property combination that includes rapid crystallization processes. In phase change alloys that are typically used for prototype and commercial applications, crystallization (or recrystallization) of amorphous bits proceeds on a nanosecond time scale.[23,24] Therefore, it is important to understand why and for which materials such fast crystallization phenomena are to be expected. Crystallization is a well understood process that is controlled by nucleation, i.e., the formation of crystalline clusters in an amorphous matrix, and subsequent growth.[25–27] Usually, crystallization of an undercooled liquid proceeds on a relatively long timescale just below the melting (or liquidus) temperature T_l[28] since the driving force for crystallization (Gibbs free energy difference between liquid and crystalline phase) is small, even though the atomic mobility is large. Close to the glass transition temperature T_g,[12] crystallization also occurs on a long timescale since the atomic mobility is low, even though the driving force for crystallization is large. The fastest crystallization of an undercooled liquid is therefore observed at some intermediate temperature T_{int}, where $T_g < T_{int} < T_l$, where a good compromise between driving force and mobility is established. While this behavior is conceptually well understood, it is usually challenging to determine experimental parameters that describe crystallization over a wide temperature range. This is in particular true for phase change materials, for which crystallization near $T = T_{int}$ occurs within timescales of as short as about 10 ns.[29] This makes it almost impossible to perform systematic measurements of crystallization parameters as a function of temperature near $T = T_{int}$. Therefore, the extrapolation of such properties from $T \sim T_g$ or $T \sim T_l$, where crystallization is slow, becomes necessary. Frequently, measurements of crystallization parameters close to T_g are performed and used to predict the crystallization behavior around T_{int} by extrapolating those parameters.[30–36]

In the present study, crystallization parameters of phase change films with different recrystallization mechanisms in laser experiments, i.e., nucleation-dominated and growth-dominated mechanisms,[29,37–39] have been determined experimentally by atomic force microscopy (AFM).[40–41] According to Refs. 29, and 37–39, $Ge_4Sb_1Te_5$ and $Ge_2Sb_2Te_5$ exhibit nucleation-dominated behavior, while $Ag_{0.055}In_{0.065}Sb_{0.59}Te_{0.29}$ (hereafter: AgIn-Sb_2Te) and $Ge_{12}Sb_{88}$ exhibit growth-dominated behavior. The 30-nm-thick thin films were sputter-deposited on a silicon wafer by direct-current magnetron sputtering.[41] The samples were annealed in a precise furnace of a power-compensated differential scanning calorimeter (DSC) around the glass transition temperature.[12,41] Several AFM scanning and annealing

cycles were alternately performed, and the annealing temperature always remained the same for the same sample. Crystallization is observed in the AFM due to the density change associated with the phase transition, which appears as a local height change.[40] Comparing crystal sizes on subsequent AFM scans at the same location revealed the crystal nucleation rate and the growth velocity. The experiment was repeated at different temperatures to determine the temperature dependence of crystal nucleation rate and growth velocity.[41] The activation energies for the growth velocity, as determined from the slopes of the straight lines in Fig. 7, appear to be in a similar range for all alloys. They are (2.90 ± 0.05) eV for AgIn-Sb_2Te, (2.74 ± 0.03) eV for $Ge_4Sb_1Te_5$, and (2.35 ± 0.05) eV for $Ge_2Sb_2Te_5$. In particular, the absolute values for the crystal growth velocities are very similar for AgIn–Sb_2Te and $Ge_4Sb_1Te_5$ for a given temperature (Fig. 7), even though these two alloys are known to exhibit a fundamentally different recrystallization mechanism in the laser experiment.[37–39] Therefore, the different recrystallization mechanisms in the laser experiment are unlikely to be a consequence of the difference in growth velocity.

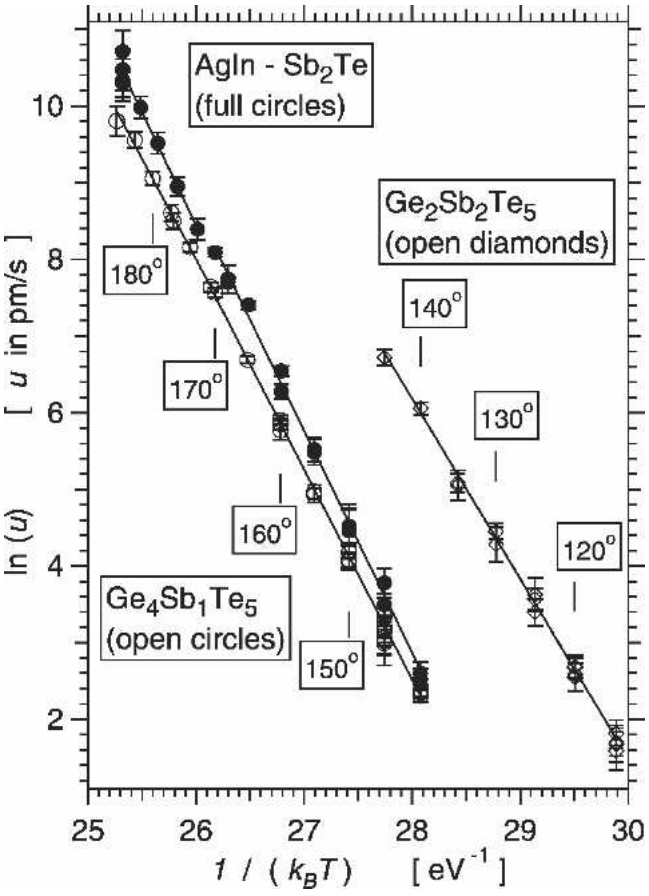

FIG. 7. Crystal growth velocity u obtained from atomic force microscopy measurements for $Ge_4Sb_1Te_5$ and $Ge_2Sb_2Te_5$ (nucleation-dominated materials in laser experiments[37–39]) and for the growth-dominated material AgIn–Sb_2Te. The activation energy for the growth velocity (which is proportional to the slope of the fitting lines) is similar for all alloys.[41]

In contrast, the nucleation rate was observed to be in line with the different recrystallization mechanisms in the laser experiment: Qualitatively, the crystal nucleation rate can be represented by the number of crystals N per unit surface area of the sample after complete crystallization of the sample surface. (Cross-sectional transmission electron microscopy showed that nucleation occurred only heterogeneously at the film surface, not at the film-substrate interface.[42]) The crystal density N is shown in Fig. 8. While N increases with increasing temperature for the GeSbTe-based alloys, it is relatively low and temperature-independent for AgIn–Sb_2Te. In conclusion, Figs. 7 and 8 show that it is a reduced nucleation rate rather than an increased growth velocity that distinguishes the growth-dominated material AgIn–Sb_2Te. More details regarding the crystal nucleation rate study can be found in Ref. 42.

Yet, this study does not answer the question why the nucleation rate is lower for AgIn–Sb_2Te than for the GeSbTe alloys. Nucleation involves the creation of an interface between the crystalline nucleus and the surrounding molten or amorphous matrix. As a consequence, the nucleation rate depends (i) on on the viscosity of the undercooled liquid (which is primarily determined by the glass transition temperature T_g), (ii) the

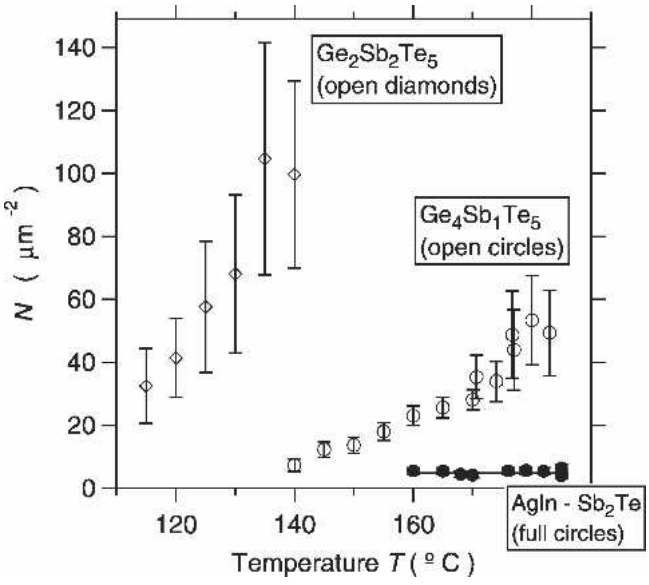

FIG. 8. Crystal density N (number of crystals per unit area after complete crystallization) obtained from AFM measurements. N is a qualitative representation of the crystal nucleation rate.[42] The nucleation behavior is in line with the recrystallization mechanism observed in laser recrystallization experiments.[37–39] The increasing crystal density with increasing temperature for the GeSbTe alloys extrapolates to a very high crystal density around $T = T_{int}$, which enables nucleation-dominated re-crystallization.

TABLE I. Lower limit for the product of α^3 (α, crystal-melt interfacial free energy) and the entropy of fusion β.

Alloy	$\alpha^3\beta$
$Ge_{12}Sb_{88}$	0.024
AgIn–Sb_2Te	0.017
$Ge_4Sb_1Te_5$	0.016
$Ge_2Sb_2Te_5$	0.008

Note: Both α and β were determined by DTA and are given as normalized and dimensionless parameters. For details, refer to Ref. 28. The higher the product $\alpha^3\beta$ is, the lower is the crystal nucleation rate. However, for a complete description of the nucleation rate, the glass transition temperature has to be taken into account as well as Ref. 12, 28.

entropy of fusion β, and (iii) the crystal-melt interfacial (free) energy α.[12,28] Values for T_g have been measured previously and found to be close to the crystallization temperature upon furnace heating.[12] The entropy of fusion β has been measured by differential thermal analysis.[28] A lower limit for the crystal-melt interfacial free energy α was estimated by undercooling liquid droplets of phase change alloys in a differential thermal analyzer (DTA) and measuring the maximum degree of undercooling upon cooling at a constant cooling rate.[28] Crystallization upon cooling was detected in the DTA by recalescence (re-heat of the droplet by the release of the heat of crystallization). The undercooling was maximized by embedding the phase change material in a liquid flux of B_2O_3. This helped to isolate the droplet from the DTA crucible walls, which could act as heterogeneous nucleation sites. Additionally, B_2O_3 eliminates nucleants from the surface of the droplet by dissolution and inclusion.[28]

Table I shows the product $\alpha^3\beta$ obtained from the DTA experiments since the crystal nucleation rate I depends on $\alpha^3\beta$, but not on α and β individually (see Ref. 28 for details). I decreases with increasing $\alpha^3\beta$, but for a complete description, the reduced glass transition temperature T_{rg} ($T_{rg} = T_g/T_l$) has to be taken into account.[12,28] There is a clear trend toward reduced values of $\alpha^3\beta$ for nucleation dominated materials such as $Ge_2Sb_2Te_5$ as compared to growth dominated alloys such as $Ge_{12}Sb_{88}$. AgIn–Sb_2Te and $Ge_4Sb_1Te_5$ exhibit similar values of $\alpha^3\beta$, but because T_{rg} is higher for AgIn–Sb_2Te than it is for $Ge_4Sb_1Te_5$, the nucleation rate for AgIn–Sb_2Te becomes significantly lower than for $Ge_4Sb_1Te_5$.[12,28]

IV. CONCLUSIONS

In summary, we have shown that the structural change in octahedral phase change alloys upon amorphization is accompanied by a substantial change in the electronic properties. This correlation between structural and electronic properties is of great importance for the application of phase change materials in electronic data storage. The unusually high vacancy concentration—e.g., 12.5% in $Ge_1Sb_2Te_4$—arises from the fact that antibonding states are occupied in the defect-free systems. Thus the creation of vacancies decreases the total energy of the system. The small energy differences between systems with different defect concentrations and their different properties allow for a systematic design of phase change alloys for data storage.

Moreover, we have shown by AFM studies of thin films of phase change materials that it is likely that the crystal nucleation rate (but not the crystal growth velocity) determines whether a phase change material crystallizes nucleation-dominated or growth-dominated during the laser-induced recrystallization of amorphous marks in a crystalline matrix. In addition, calorimetry studies have answered the question why the nucleation rate is higher for nucleation-dominated materials than for growth-dominated materials: It was found that the nucleation-dominated materials are characterized by lower values of crystal-melt interfacial energy, entropy of fusion, and reduced glass transition temperature.

ACKNOWLEDGMENTS

Financial support by the 6th Framework Program of the European Commission within the CAMELS-Project (Contract No. IST-3-017406) is gratefully acknowledged. Furthermore, we would like to thank R. Dronskowski and M. Gillessen from the Institut für Anorganische Chemie of the RWTH Aachen for fruitful discussions. One of the authors (J.A. Kalb) acknowledges the Studienstiftung des Deutschen Volkes and the Deutscher Akademischer Auslandsdienst for financial support.

REFERENCES

1. S.R. Ovshinsky: Reversible electrical switching phenomena in disordered structures. *Phys. Rev. Lett.* **21,** 1450 (1968).
2. G. Zhou: Material aspects in phase change optical recording. *Mater. Sci. Eng., A* **304–306,** 73 (2001).
3. M. Wuttig: Phase-change materials—Towards a universal memory? *Nat. Mater.* **4,** 265 (2005).
4. N. Yamada: Erasable phase-change optical materials. *MRS Bull.* **21(9),** 48 (1996).
5. I. Friedrich, V. Weidenhof, W. Njoroge, P. Franz, and M. Wuttig: Structural transformations of $Ge_2Sb_2Te_5$ films studied by electrical resistance measurements. *J. Appl. Phys.* **87,** 4130 (2000).
6. M. Lankhorst, B. Ketelaars, and R. Wolters: Low-cost and nanoscale non-volatile memory concept for future silicon chips. *Nat. Mater.* **4,** 347 (2005).
7. H.R. Philipp and H. Ehrenreich: Optical properties of semiconductors. *Phys. Rev.* **129,** 1550 (1963).
8. J. Stuke and G. Zimmerer: Optical properties of amorphous 3–5 compounds. 1. Experiment. *Phys. Status Solidi B—Basic Res.* **49,** 513 (1972).
9. W. Wełnic, S. Botti, L. Reining, and M.Wuttig: Origin of the

optical contrast in phase change materials. *Phys. Rev. Lett.* **98,** 236403 (2007).
10. A.V. Kolobov, P. Fons, J. Tominaga, A.L. Ankudinov, S.N. Yannopoulos, and K.S. Andikopoulos: Crystallization-induced short-range order changes in amorphous GeTe. *J. Phys. Condens. Matter.* **16,** 5103 (2004).
11. A.V. Kolobov, P. Fons, A.I. Frenkel, A.L. Ankudinov, J. Tominaga, and T. Urugal: Understanding the phase-change mechanism of rewritable optical media. *Nat. Mater.* **3,** 703 (2004).
12. J. Kalb, M. Wuttig, and F. Spaepen: Calorimetric measurements of structural relaxation and glass transition temperatures in sputtered films of amorphous Te alloys used for phase change recording. *J. Mater. Res.* **22,** 748 (2007).
13. W. Wełnic, A. Pamungkas, R. Detemple, C. Steimer, S. Blûgui, and M. Wuttig: Unraveling the interplay of local structure and physical properties in phase-change materials. *Nat. Mater.* **5,** 56 (2006).
14. M. Luo and M. Wuttig: The dependence of crystal structure of Te-based phase-change materials on the number of valence electrons. *Adv. Mat.* **16,** 439 (2004).
15. R. Peierls: *Quantum Theory of Solids* (Oxford University Press, Oxford, UK, 1956).
16. M. Wuttig, D. Lüsebrink, D. Wamwangi, W. Wełnic, M. Gilleßen, and R. Dronskowski: The role of vacancies and local distortions in the design of new phase change materials. *Nat. Mater.* **6,** 122 (2007).
17. T. Matsunaga, Y. Kubota, and N. Yamada: Structures of stable and metastable $Ge_2Sb_2Te_5$, an intermetallic compound in the GeTe-Sb_2Te_3 pseudobinary systems. *Acta Crystallogr. B* **60,** 685 (2004).
18. T. Matsunaga, R. Kojima, N. Yamada, K. Kifune, Y. Kubote, Y. Tabata, and M. Takata: Single structure widely distributed in a GeTe-Sb_2Te_3 pseudobinary system: A rocksalt structure is retained by intrinsically containing an enormous number of vacancies within its crystal. *Inorg. Chem.* **45,** 2235 (2006).
19. S. Shamoto, T. Matsumaga, N. Yamada, Th. Proffen, J.W. Richardson, Jr., J.H. Chung, and T. Egani: Large displacement of germanium atoms in crystalline $Ge_2Sb_2Te_5$. *Appl. Phys. Lett.* **86,** 081904 (2005).
20. F. El-Mellouhi, N. Mousseau, and P. Ordejon: Sampling the diffusion paths of a neutral vacancy in silicon with quantum mechanical calculations. *Phys. Rev. B* **70,** 205202 (2004).
21. J-P. Gaspard and R. Ceolin: Hume-rothery rule in v-vi compounds. *Solid State Comm.* **84,** 839 (1992).
22. J-P. Gaspard, A. Pellegatti, F. Marinelli, and C. Bichara: Peierls instabilities in covalent structures I. Electronic structure, cohesion and the Z = 8–N rule. *Philos. Mag. B* **77,** 727 (1998).
23. N. Yamada, E. Ohno, K. Nishiuchi, N. Akahira, and M. Takao: Rapid phase transitions of GeTe-Sb_2Te_3 pseudobinary amorphous thin films for an optical disk memory. *J. Appl. Phys.* **69,** 2849 (1991).
24. S. Hudgens and B. Johnson: Overview of phase-change chalcogenide nonvolatile memory technology. *MRS Bull.* **29(11),** 829 (2004).
25. J. Christian: *Transformation in Metals and Alloys*, 2nd ed. (Pergamon Press, Oxford, UK, 1975).
26. D. Herlach: Non-equilibrium solidification of undercooled metallic melts. *Mater. Sci. Eng., R* **12,** 177 (1994).
27. K. Kelton: Crystal nucleation in liquids and glasses. *Solid State Phys.* **45,** 75 (1991).
28. J. Kalb, F. Spaepen, and M. Wuttig: Kinetics of crystal nucleation in undercooled droplets of Sb- and Te-based alloys used for phase change recording. *J. Appl. Phys.* **98,** 054910 (2005).
29. V. Weidenhof, I. Friedrich, S. Ziegler, and M. Wuttig: Laser induced crystallization of amorphous $Ge_2Sb_2Te_5$ films. *J. Appl. Phys.* **89,** 3168 (2001).
30. G. Ruitenberg, A. Petford-Long, and R. Doole: Determination of the isothermal nucleation and growth parameters for the crystallization of thin $Ge_2Sb_2Te_5$ films. *J. Appl. Phys.* **92,** 3116 (2002).
31. S. Privitera, C. Bongiorno, E. Rimini, and R. Zonca: Crystal nucleation and growth processes in $Ge_2Sb_2Te_5$. *Appl. Phys. Lett.* **84,** 4448 (2004).
32. B. Kooi and J.D. Hosson: On the crystallization of thin films composed of $Sb_{3.6}Te$ with Ge for rewritable data storage. *J. Appl. Phys.* **95,** 4714 (2004).
33. C. Peng, L. Cheng, and M. Mansuripur: Experimental and theoretical investigations of laser-induced crystallization and amorphization in phase-change optical-recording media. *J. Appl. Phys.* **82,** 4183 (1997).
34. S. Senkader and C. Wright: Models for phase-change of $Ge_2Sb_2Te_5$ in optical and electrical memory devices. *J. Appl. Phys.* **95,** 504 (2004).
35. A. Sheila and T. Schlesinger: Modeling thermal cross talk and overwrite jitter in growth dominant phase change optical-recording media at high data rates. *J. Appl. Phys.* **91,** 2803 (2002).
36. E. Meinders, H. Borg, M. Lankhorst, J. Hellmig, and A. Mijiritskii: Numerical simulation of mark formation in dual-stack phase-change recording. *J. Appl. Phys.* **91,** 9794 (2002).
37. J. Coombs, A. Jongenelis, W. van Es-Spiekman, and B. Jacobs: Laser-induced crystallization phenomena in GeTe-based alloys. ii. Composition dependence of nucleation and growth. *J. Appl. Phys.* **82,** 4183 (1997).
38. H.J. Borg, M. Van Schijndel, J.C.N. Rijpers, H.H.R. Lankhoist, G. Zhou, M.J. Dekker, I.P.D. Ubbens, and M. Kuijper: Phase-change media for high-numericalaperture and blue-wavelength recording. *Jap. J. Appl. Phys.* **40,** 1592 (2001).
39. L. van Pieterson, M. van Schijndel, J. Rijpers, and M. Kaiser: Te-free, Sb-based phase-change materials for high-speed rewritable optical recording. *Appl. Phys. Lett.* **83,** 1373 (2003).
40. V. Weidenhof, I. Friedrich, S. Ziegler, and M. Wuttig: Atomic force microscopy study of laser induced phase transitions in $Ge_2Sb_2Te_5$. *J. Appl. Phys.* **86,** 5879 (1999).
41. J. Kalb, F. Spaepen, and M. Wuttig: Atomic force microscopy measurements of crystal nucleation and growth rates in thin films of amorphous Te alloys. *Appl. Phys. Lett.* **84,** 5240 (2004).
42. J. Kalb, C. Wen, F. Spaepen, H. Dieker, and M. Wuttig: Crystal morphology and nucleation in thin films of amorphous Te alloys used for phase change recording. *J. Appl. Phys.* **98,** 054902 (2005).